

## Photon Multiplicity Measurements : From SPS to RHIC and LHC

Bedangadas Mohanty

Institute of Physics, Bhuaneswar 751005, India

e-mail : bedanga@iopb.res.in

**Abstract.** Results from the photon multiplicity measurements using a fine granularity preshower photon multiplicity detector (PMD) at CERN SPS are discussed. These include study of pseudo-rapidity distributions of photons, scaling of photon multiplicity with number of participating nucleons, centrality dependence of  $\langle p_T \rangle$  of photons, event-by-event fluctuations in photon multiplicity and localised charged-neutral fluctuations. Basic features of the PMD to be used in STAR experiment at RHIC and in ALICE experiment at LHC are also discussed.

**Keywords.** Photon multiplicity detector; heavy-ion collisions; Quark-Gluon Plasma; pseudo-rapidity distribution; disoriented chiral condensates, scaling; event-by-event fluctuations

**PACS Nos** 25.75.-q;25.75.Dw;25.75.Gz

### 1. Introduction

Measurement of photon multiplicity in relativistic heavy-ion collisions is complimentary to the well established methods of charged hadron measurements and it shows a great promise in studying the various aspects of the reaction mechanism of phase transition from hadronic matter to Quark-Gluon Plasma and dynamics of particle production. In heavy-ion collisions it is important to correlate information obtained from various global observables (such as charged particle multiplicity, mean transverse momentum ( $\langle p_T \rangle$ ) and transverse energy ( $E_T$ )) for proper understanding of the physics processes occurring in the reaction. Photon multiplicity is an additional global observable. More specifically photon multiplicity provides an unique opportunity to study the changes in the relative population of the electromagnetic and hadronic components of the multi-particle final state. These and several other aspects are discussed in this paper.

The paper is organised as follows, first we give a brief description of the photon multiplicity detectors (PMD) used at SPS experiments. In section 3 we discuss the various physics issues addressed by the PMD at SPS, such as the study of pseudo-rapidity distribution of photons ( $dN_\gamma/d\eta$ ), scaling of total number of photons with number of participating nucleons, measurement of event-by-event mean transverse momentum ( $\langle p_T \rangle$ ) of photons, event-by-event fluctuation in photon multiplicity and search for domains of disoriented chiral condensates (DCC) through the study of localised charged-neutral fluctuations. A comparison to the results from charged particles will be made wherever possible. The

study of azimuthal anisotropy of photons is covered in an separate article in this volume. In section 4 we discuss the PMD to be installed in STAR experiment at RHIC and ALICE experiment at LHC. This is followed by a summary in the last section.

## 2. Photon multiplicity detectors at CERN SPS

A fine granularity preshower PMD was implemented in the WA93 experiment at CERN SPS [], allowing the *first ever* measurement of multiplicity, rapidity and azimuthal distributions of photons in ultra-relativistic heavy-ion collisions. The basic features of the detector are given in Table 1. The minimum bias distribution of the photon multiplicity as measured by the PMD for S + Au at 200 AGeV in WA93 experiment is shown in Figure 1. The distribution has been obtained for the full azimuthal coverage of the PMD and has been compared to results obtained from the VENUS event generator. It is observed that VENUS under predicts photon multiplicity for central events. Subsequently a similar PMD was also installed in the WA98 experiment []. The basic features of the PMD in WA98 experiment are also given in Table 1. The minimum bias distribution of photon multiplicity as measured by the PMD in WA98 experiment is shown in Figure 1. The experimental results for different target ions has been compared to those obtained from the VENUS event generator. VENUS is found to under predict photon multiplicity for central collisions, and it under predicts more for asymmetric ion collisions (Pb + Nb and Pb + Ni).

**Table 1.** PMD in WA93 and WA98 experiments

Basic features	WA93	WA98
Data taking	1991 and 1992	1994-1996
Beam and target	S + Au & S + S	Pb + Pb, Pb + Ni & Pb + Nb
Energy	200 A GeV	158 A GeV
No. of scintillator pads	7600	53000
Readout	CCD camera	CCD camera
Distance from target	10.09 m	21.5 m
$\eta$ coverage	2.8 - 5.2	2.5 - 4.2
$\eta$ coverage with full $\phi$	3.3 - 4.8	3.2 - 4.0
$p_T$ acceptance	$\geq 20$ MeV/c	$\geq 30$ MeV/c
Photon counting Efficiency (central to peripheral)	65 - 75%	68 - 73 %
Purity of photon sample(central to peripheral)	70%	65 - 54 %

Both WA93 and WA98 experiments include several other detectors for charged particle multiplicity and momentum measurements along with trigger detectors for defining the centrality of the reaction. The common coverage of the charged particle multiplicity detector and the calorimeter (for measuring  $E_T$ ) with PMD was used for event-by-event measurement of  $\langle p_T \rangle$  of photons and search for possible formation of DCC.

## 3. Physics issues addressed by PMD at SPS

In this section we discuss the various physics issues addressed by the PMD at CERN SPS. These includes study of  $dN_\gamma/d\eta$ , scaling of photons, event-by-event  $\langle p_T \rangle$  of photons, event-by-event fluctuation in photon multiplicity and formation of DCC.

Photon multiplicity Measurements...

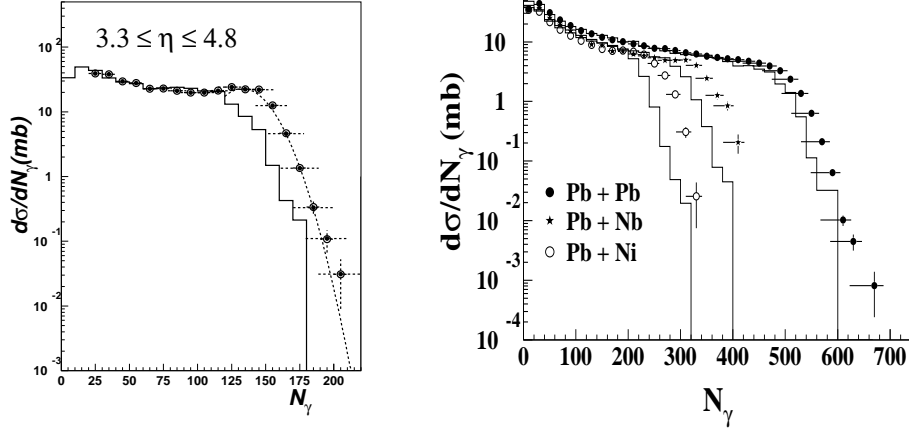


**Figure 1.** Minimum bias inclusive photon cross sections for S+Au reaction at 200-AGeV (left plot) and for Pb+Ni, Pb+Nb, and Pb+Pb reactions at 158-AGeV (right plot). Solid histograms are the corresponding distributions obtained from the VENUS event generator.

### 3.1 Pseudo-rapidity distribution of photons

One of the challenges in relativistic heavy-ion collisions is the large number of particles produced. Measurement of particle density in rapidity is a convenient way to describe heavy-ion collisions. It has also been suggested that fluctuations in pseudo-rapidity distributions is a signature of phase transition from hadronic matter to Quark-Gluon plasma. Further, pseudo-rapidity density can be related to a thermodynamic quantity, entropy density, in heavy-ion collisions. All these motivate us to study the pseudo-rapidity distributions of photons ( $dN_\gamma/d\eta$ ). We have studied  $dN_\gamma/d\eta$  in WA93 and WA98 experiments at CERN SPS [1]. These distributions for S + Au and Pb + Pb reactions for different centrality classes are shown in Figure 2. They are found to be good gaussians. The results from VENUS are also shown in the figures. One observes that VENUS under predicts data for central collisions.

The best way to study the pseudo-rapidity distributions is to look at the shape parameters of the distributions. The shape parameters are the pseudo-rapidity density at mid-rapidity ( $\rho_{max}$ ), width of the pseudo-rapidity distribution ( $\sigma$ ) and pseudo-rapidity peak ( $\eta_{peak}$ ). These are shown in Figure 3 as a function of transverse energy and number of participating nucleons for WA93 and WA98 experiments respectively. The results have been compared to those obtained from VENUS event generator. The pseudo-rapidity density at mid-rapidity is found to increase with increase in centrality, which can be understood from simple geometrical picture of the collision. Results from VENUS is also found to follow the similar trend. For higher centrality of the reaction VENUS under predicts the data. The width of the pseudo-rapidity distributions for various centrality classes are found to be similar within the quoted errors and the trend is well explained by results from VENUS. The pseudo-rapidity peak for the WA98 experiment was found to be 2.92.

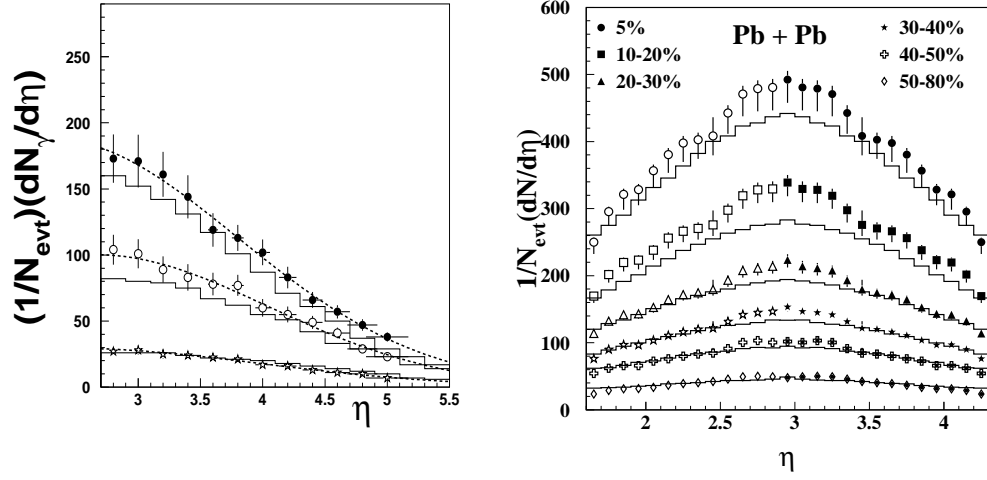


**Figure 2.** Pseudo-rapidity distributions of photons for S+Au reaction at 200-AGeV (left plot) and Pb+Pb reaction at 158-AGeV (right plot). The solid histograms are the corresponding distributions obtained from the VENUS event generator.

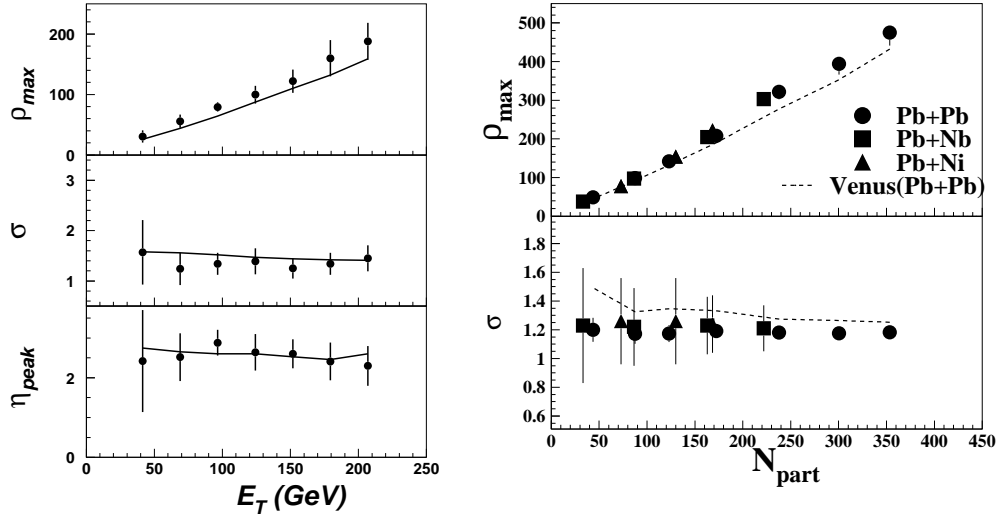


**Figure 3.** Pseudo-rapidity density ( $\rho_{max}$ ), and width of the pseudo-rapidity distribution ( $\sigma$ ) are shown as a function of centrality of the reaction (defined through the  $E_T$  values for WA93 results (left plot) and number of participating nucleons for WA98 results (right plot)).

### 3.2 Scaling of photons

It is important to study the scaling of particle multiplicity as they test the various models for particle production. Also various experimental signatures require comparison of observables of different system sizes, hence a proper understanding of scaling is essential. While scaling with number of collisions arises naturally in a picture of a superposition of nucleon-nucleon collisions, with possible modifications by initial state effects, the participant scaling is more naturally related to a system with strong final state re-scattering, where the incoming particles lose their memory and every participant contributes a similar amount of energy. The scaling behavior can therefore carry important information on the reaction dynamics. It is therefore of interest to study the scaling properties with respect to number of participants or collisions. We have studied the scaling of total number of photons with number of participating nucleons [1]. The results for photons from Pb+Pb collisions at 158-AGeV are shown in Figure 4. Fitting the data points to the function  $C \times N_{part}^\alpha$ , yields the value of  $\alpha$  to be  $1.12 \pm 0.03$ . Similar analysis for charged particles in the same experiment and using the data from the silicon pad multiplicity detector gives a value of  $\alpha = 1.07 \pm 0.05$  [1]. Within the quoted systematic errors the value of  $\alpha$  are similar for both photons and charged particles and indicates a deviation from the picture of a naive Wounded Nucleon Model ( $\alpha = 1$ ).

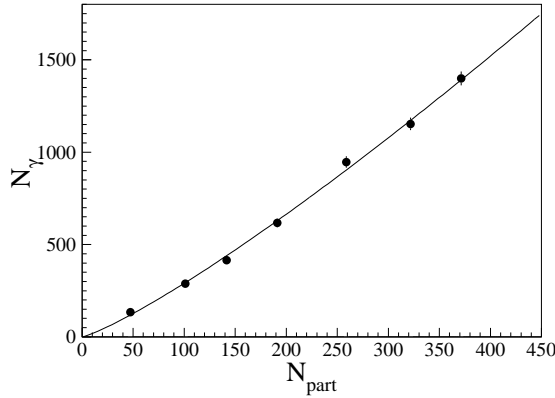


**Figure 4.** Scaling behavior of photons. Integrated number of photons are plotted as a function of number of participating nucleons. The solid lines show power-law fit to the data, which yields the value of exponent,  $\alpha = 1.12 \pm 0.03$ .

### 3.3 Event-by-event mean transverse momentum of photons

Variation of  $\langle p_T \rangle$  of produced particles with global multiplicity could provide signature of phase transition from hadronic matter to Quark-Gluon plasma. The expected behavior will be similar to that of variation of entropy density with temperature, where temperature increases with increase in entropy density before phase transition then remains unchanged

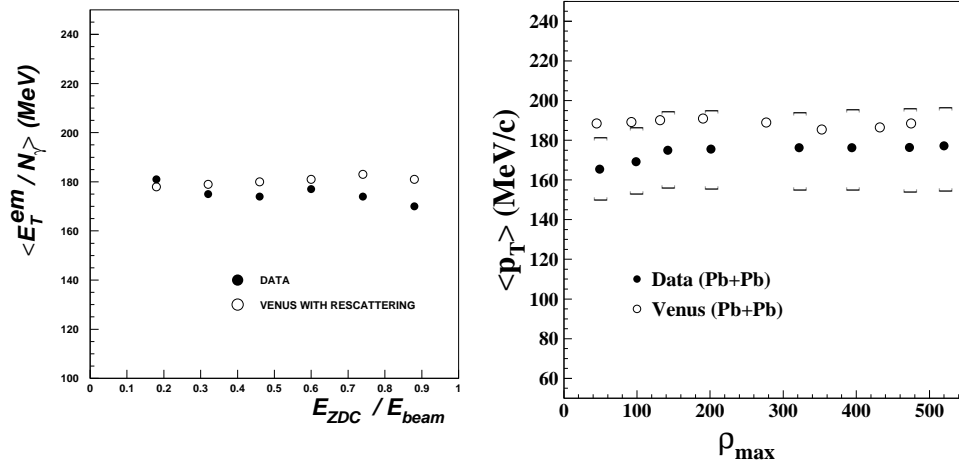


**Figure 5.** The mean transverse momentum,  $\langle p_T \rangle$ , of photons as a function of centrality. For the S+Au collisions (left plot) centrality is defined by  $E_{ZDC}/E_{beam}$  for the Pb+Pb collisions it is defined through the pseudo-rapidity density of photons at mid-rapidity,  $\rho_{max}$ . The  $\langle p_T \rangle$  values obtained from the VENUS event generator are superimposed for comparison.

during the transition and finally again increases with entropy density after phase transition. Entropy density is related to pseudo-rapidity density and transverse momentum to temperature. Hence a study of variation of transverse momentum with pseudo-rapidity density (or centrality of reaction) can be an experimental signature of QGP formation.

We have measured event-by-event  $\langle p_T \rangle$  of photons in both WA93 [1] and WA98 experiments [2], using the relation  $\langle p_T \rangle = E_T^{em} / N_\gamma$ . Where  $E_T^{em}$  is the transverse component of the electromagnetic energy measured in the mid-rapidity calorimeter, and  $N_\gamma$  is the number of photons measured by PMD in a given common  $\eta$ - $\phi$  region of the two detectors. The results are shown in the Figure 5. One observes that for both WA93 and WA98 experiment, the  $\langle p_T \rangle$  values are constant as a function of centrality of the reaction within the quoted systematic errors and agrees well with those obtained from VENUS.

### 3.4 Event-by-event fluctuation in photon multiplicity

Event-by-event fluctuations in global observables such as photon multiplicity has generated lot of interest in recent years [3]. This is because fluctuations in the global observables are related to thermodynamical properties of matter, more specifically multiplicity fluctuations can be related to matter compressibility. Further studying the centrality and rapidity acceptance of fluctuations can help in finding the possible existence of the *tri-critical* point in the QCD phase diagram [4]. We have studied the centrality dependence and rapidity dependence of fluctuations in photons and the results are shown in Figure 6 [5]. The fluctuation in photon multiplicity ( $\omega_\gamma$ ) is defined by the relation  $\omega_\gamma = \sigma_\gamma^2 / \langle N_\gamma \rangle$ . Where  $\sigma_\gamma$  is the standard deviation and  $\langle N_\gamma \rangle$  the mean of the gaussian photon multiplicity distribution for a particular centrality class. For results on the centrality dependence of photon

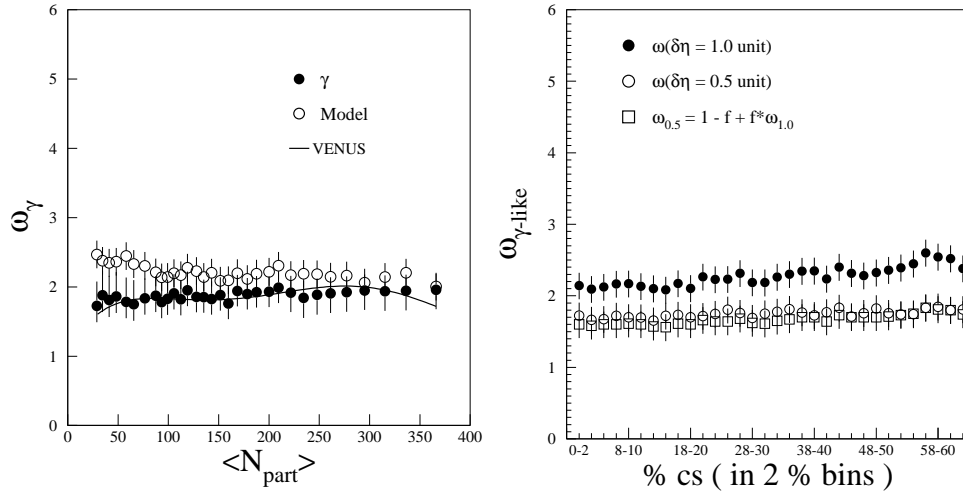


**Figure 6.** Left plot : Relative fluctuations,  $\omega_\gamma$  of photons as a function of number of participants. These are compared to calculations from a participant model and those from VENUS event generator. Right plot : Photon multiplicity fluctuations for two  $\eta$  acceptance selections. The open squares represent estimated values of fluctuations in 0.5 unit of  $\Delta\eta$  from the observed fluctuations in 1.0 unit  $\Delta\eta$ .  $f$  is the ratio of mean photon multiplicity for 0.5 unit of  $\Delta\eta$  to that for 1.0 unit of  $\Delta\eta$ .

multiplicity fluctuation the data has been compared to the results obtained from VENUS event generator and a simple participant model. The results of fluctuation in photon data are presented as a function of mean number of participant nucleon and are found to be in agreement with those from the model calculations within the quoted systematic errors. For the rapidity acceptance studies, the decrease in fluctuation with decrease in acceptance has been explained using a simple statistical model. The model assumes that the distribution of particles in a smaller rapidity window  $\Delta\eta$  follows a binomial sampling []. The results have been presented as a function of 2% bins in cross section of total transverse energy.

### 3.5 Formation of Disoriented chiral condensates at SPS

The formation of hot and dense matter in high energy heavy-ion collisions has the possibility of creating a chiral symmetry restored phase in the laboratory. A consequence of this is the possibility of the formation of disoriented chiral condensate (DCC) []. The detection and study of DCC is expected to provide valuable information about the chiral phase transition and vacuum structure of strong interactions.

DCC formation in a given domain would be associated with large event-by-event fluctuation in the ratio of neutral to charged pions in a certain domain. Since neutral pions decay to photons and majority of the charged pions are charged pions. The experimental signature of formation of DCC would be large event-by-event localised fluctuation in ratio of photons to charged particles. Following this theoretical predictions, WA98 recently carried out a detailed study of central Pb+Pb events and has been published in Ref. [].

**Table 2.** Type of fluctuations preserved by various mixed events

Fluctuation	Mixed		Event	
	M1	M2	M3-ch	M3- $\gamma$
$N_\gamma$ -only	No	Yes	Yes	No
$N_{ch}$ - only	No	Yes	No	Yes
correlated $N_\gamma$ - $N_{ch}$	No	No	No	No

The data presented here were taken during December 1996 at CERN SPS with 158-A GeV Pb ion beam on a Pb target of thickness 213  $\mu\text{m}$ . The Goliath magnet was kept off during these runs. A total of 85K central events, corresponding to the top 5% of the minimum bias cross section as determined from the total transverse energy measured by the mid-rapidity calorimeter (MIRAC), are analyzed. The analyzed data corresponds to a common  $\eta$  ( $2.9 < \eta < 3.75$ ) and  $\phi$  coverage of charged particle and photon multiplicity detectors and for different segments in azimuth ( $\phi$ ).

The measured results are interpreted by comparison with simulated events and with several types of mixed events. Simulated events were generated using the VENUS 4.12 event generator with default parameters. The output was processed through a WA98 detector simulation package in the GEANT 3.21 framework. Due to the inherent uncertainties in the description of “normal” physics and detector response in the VENUS+GEANT simulations, the observation of an experimental result which differs from the case with zero DCC fraction in simulation cannot be taken alone as evidence of DCC observation. For this reason four different types of mixed events have been created from the real events in order to search for non-statistical fluctuations by removing various correlations in a controlled manner while preserving the characteristics of the measured distributions as accurately as possible. The first type of mixed events (M1), are generated by mixing hits in both the PMD and SPMD separately, with no two hits taken from the same event. Hits within a detector in the mixed events are not allowed to lie within the two track resolution of that detector. The second kind of mixed events (M2) are generated by mixing the unaltered PMD hits of one event with the unaltered SPMD hits of a different event. Intermediate between the M1 and M2 kinds of mixed events is the case where the hits within the PMD are unaltered while the SPMD hits are mixed (M3- $\gamma$ ), or the SPMD hits are unaltered while the PMD hits are mixed (M3-ch). In each type of mixed event the global (bin 1)  $N_{\gamma\text{-like}}-N_{ch}$  correlation is maintained as in the real event. The specific physics issues probed by each mixed event are tabulated in Table 2.

In order to look for any possible localized fluctuation in photon and charged particle multiplicities, which may have non-statistical origin, it is necessary to look at the correlation between  $N_{\gamma\text{-like}}$  and  $N_{ch}$  at various segmentation in  $\eta$  and  $\phi$ . Event-by-event correlation between  $N_{\gamma\text{-like}}$  and  $N_{ch}$  has been studied in  $\phi$ -segments, by dividing the entire  $\phi$ -space into 2, 4, 8 and 16 bins. Fig. 7 shows the scatter plots of  $N_{\gamma\text{-like}}$  and  $N_{ch}$  distributions. The correlation plot for each of the  $\phi$  segments, starting with the case of 1 bin which corresponds to no segmentation are also shown. A common correlation axis ( $Z$ ) has been obtained for the full distribution by fitting the  $N_{\gamma\text{-like}}$  and  $N_{ch}$  correlation with a second order polynomial. The correlation axis with fit parameters are shown in the figures. The distances of separation ( $D_Z$ ) between the data points and the correlation axis have been calculated with the convention that  $D_Z$  is positive for points below the  $Z$ -axis. The distribution of  $D_Z$  represents the relative fluctuations of  $N_{\gamma\text{-like}}$  and  $N_{ch}$  from the correlation axis at any given  $\phi$  bin. In order to compare the fluctuations for different  $\phi$  bins



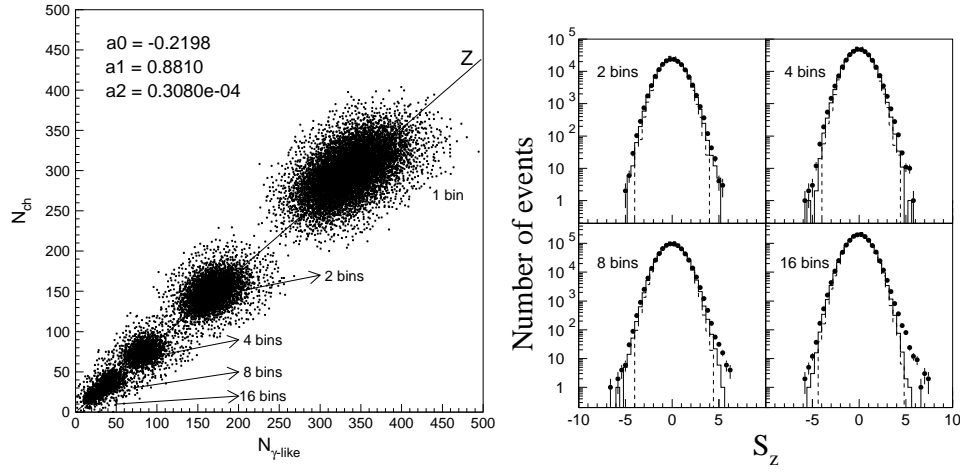


**Figure 7.** Left plot : Scatter plot showing the correlation of  $N_{\gamma\text{-like}}$  and  $N_{\text{ch}}$  for 1,2,4,8 and 16 bins in azimuthal angle,  $\phi$ , for the common coverage of the PMD and SPMD. The common correlation axis ( $Z$ ) obtained by fitting the distributions to a second order polynomial is also shown along with the fit parameters. Right plot : The  $S_Z$  distributions for data (solid circles), M1 mixed events (solid histogram) and simulated events (dashed histogram) for various bins in azimuthal angle. Distributions of other mixed events are not shown for clarity of presentation.

in the same level, we use a scaled variable,  $S_Z = D_Z/s(D_Z)$ , where  $s(D_Z)$  represents the rms deviation of the  $D_Z$  distribution for VENUS events, obtained in a similar manner. The presence of events with localized fluctuations in  $N_{\gamma\text{-like}}$  and  $N_{\text{ch}}$ , at a given  $\phi$  bin, is expected to result in a broader distribution of  $S_Z$  compared to those for normal events at that particular bin. For comparison,  $S_Z$  distributions are also obtained for mixed events.

The  $S_Z$  distributions calculated at different  $\phi$  bins are shown in Fig. 7 for data, M1, and VENUS events. The distributions for other mixed events are not shown for clarity of presentation. The small differences in the  $S_Z$  distributions have been quantified in terms of the corresponding rms deviations of these distributions as shown in Fig. 8. The statistical errors on the values are small and are within the sizes of the symbol. The bars represent statistical and systematic errors added in quadrature. The rms deviations of M2-type of mixed events are found to agree with those of the experimental data within errors. Thereby suggesting the absence of event-by-event localized correlated fluctuations in  $N_{\gamma\text{-like}}$  and  $N_{\text{ch}}$  or DCC-type fluctuations. The rms deviations of M1-type of mixed events are found to be lower than those obtained for data for 2, 4 and 8 bins in  $\phi$ . The results form M3-type of mixed events are found in between those obtained form data and M1-type mixed events.

These results indicate the presence of localized fluctuations in data, due to both photons and charged particles for certain bins in  $\phi$ . Within the context of a simple DCC model [], upper limits on the presence of localized non-statistical DCC-like fluctuations has been set to be  $10^{-2}$  for DCC domain size with  $\Delta\phi$  between  $45\text{--}90^\circ$  and  $3 \times 10^{-3}$  for  $\Delta\phi$  between  $90\text{--}135^\circ$  with 90% confidence level.

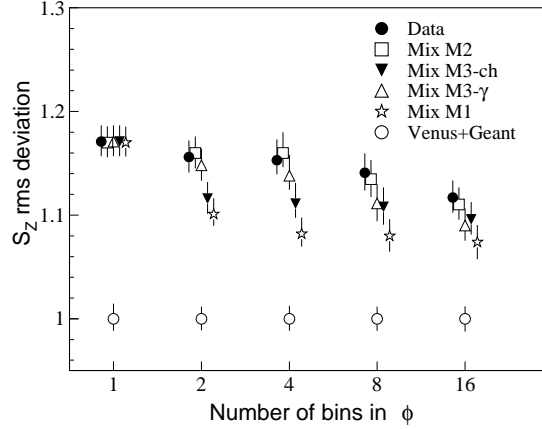


**Figure 8.** The root mean square (rms) deviations of the  $S_z$  distributions for data, mixed events and simulated events as a function of number of bins in azimuthal angle.

#### 4. Photon multiplicity detectors at RHIC and LHC

Photon multiplicity detectors will be installed in STAR experiment at RHIC and in ALICE at LHC. The detector technology is different from those used at SPS. PMD in STAR and ALICE will be a gas based detector with honeycomb cells []. Typical detector parameters for the PMD to be used in STAR and ALICE is given in the Table 3.

**Table 3.** PMD in STAR and ALICE

Basic features	STAR-PMD	ALICE-PMD
Expected year of Installation	2002	2005 - 2006
Beam and target	Au + Au	Pb + Pb
CMS Energy	200 A GeV	5.5 A TeV
No. channels	82944	270,000
Readout	Gassiplex+CRAMS	Gassiplex+CRAMS
Distance from target	5.5 m	3.5 m
$\eta$ coverage	2.3 - 3.9	2.3 - 3.5
Efficiency (central)	62 %	64 %
Purity (central)	61%	60 %

PMD will address all the physics issues discussed in Section 3. It will have overlap of about one unit in  $\eta$  with full  $\phi$  with the forward time projection chamber (FTPC) in STAR. The momentum information of charged particles in FTPC will strengthen the DCC-type of study at RHIC. This is demonstrated by a simple calculation given below. In addition, PMD will be able to give estimates of transverse electromagnetic energy in ALICE. High multiplicity environment at ALICE will be suitable for such estimates as the statistical fluctuations on transverse electromagnetic energy measurements gets reduced.

## 4.1 DCC search in STAR

The  $p_T$  information of charged particles will enhance the possibility of DCC search and verify the various features of DCC domain, such as DCC-pions are low  $p_T$  pions and DCC formation may lead to low  $p_T$  enhancement in pions. The photon multiplicity detector in-conjunction with a charged particle detectors which gives multiplicity along with particle-wise momentum information, such as the FTPC in STAR experiment can be used.

In order to show the utility of  $p_T$  information we carried out the following simulation study. The basic detector setup for DCC study was implemented by putting a photon multiplicity detector and a charged particle multiplicity detector with momentum information, having a common coverage (as in STAR ) with realistic detector parameters. The photon counting efficiency was taken as  $70\% \pm 5\%$  and contamination in photon sample was taken to be  $30\% \pm 5\%$ . The detectors accepts particles with momentum above  $30 \text{ MeV}/c$ . The efficiency of charged particle detector was taken as  $90\% \pm 5\%$  with  $p_T$  resolution of  $\frac{\Delta p_T}{p_T} = 0.2$ . Then a DCC-type fluctuations in low  $p_T$  pions was introduced through a simple DCC model as described in Ref. []. Events with different fractions of DCC-type events were generated by mixing normal events and DCC-type events. Then the resultant events were analysed using DWT analysis. The analysis was done with and without  $p_T$  cut on charged particle data ( $p_T \geq 150 \text{ MeV}/c$ ). The results are shown in Figure 9. One finds the strength,  $\zeta$ , of the DCC signal as a function of percentage of events being DCC-type is higher with  $p_T$  cut than without  $p_T$  cut. This clearly demonstrated that with  $p_T$  information of charged particles the sensitivity to search for DCC at RHIC increases.

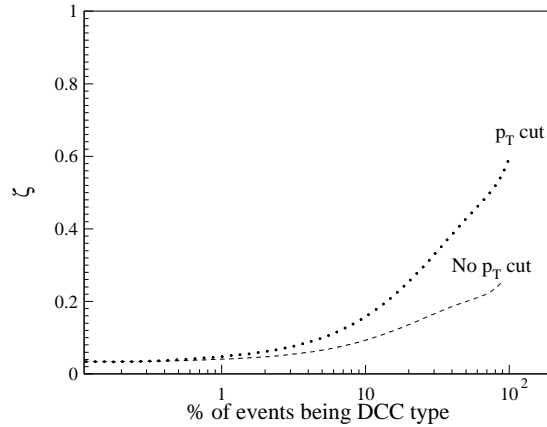


**Figure 9.** Variation of  $\zeta$  as a function of % of events being DCC-type, for charged particle detector with  $p_T$  information. Also shown are the corresponding results with charged particle detector without  $p_T$  information.

## 5. Summary

A high granularity preshower photon multiplicity detector was successfully implemented in the WA93 and WA98 experiments at CERN SPS. The PMD provided the *first ever* measurement of multiplicity, rapidity and azimuthal distributions of photons in ultra-relativistic heavy-ion collisions. Analysis of these distributions showed that photon multiplicity is an important global observable, providing significant information regarding particle production and reaction mechanism in heavy-ion collisions at relativistic energies. The study of pseudo-rapidity distributions of photons, event-by-event measurement of mean transverse momentum of photons, scaling of photons and event-by-event fluctuations in photon multiplicity suggest that it is complementary to charged particle measurements. In addition to this, correlation between photon and charged particle multiplicity has been found to provide important information regarding formation of DCC in relativistic heavy-ion collisions. A gas based PMD will be implemented in the STAR experiment at RHIC and in ALICE experiment at LHC. It will address all the physics issues, which were studied using the PMD at CERN SPS. However, DCC search will get a boost due to momentum information of charged particles at STAR. With very high multiplicity environment at ALICE, PMD can provide estimates of transverse electromagnetic energy at LHC.

### Acknowledgments

We wish to thank all the collaborators of WA93 and WA98 experiments for their active participation in the analysis of data from PMD, which resulted in many good publications, most of which is discussed in this work. We also wish to thank our STAR and ALICE Collaborators who have contributed to the proposed use of PMD in these experiments. We acknowledge with appreciation the effort of all engineers, technicians, and support staff who have participated in the construction of the photon multiplicity detector and running of the WA93 and WA98 experiments. This work was supported jointly by the Department of Atomic Energy, the Department of Science and Technology, the Council of Scientific and Industrial Research and the University Grants Commission of the Government of India.

### References

- [1] M. M. Aggarwal et al., Nucl. Instr. and Meth. in Phys. Res. **A372** (1996) 143.
- [2] M.M. Aggarwal et al., Nucl. Instr. and Methods in Phys. Res. **A424** (1999) 395.
- [3] M.M. Aggarwal et al., (WA93 Collaboration), Phys. Rev. **C58** (1998) 1146.
- [4] M.M. Aggarwal et al., (WA98 Collaboration), Phys. Lett. **B458** (1999) 422.
- [5] M.M. Aggarwal et al., (WA98 Collaboration), Eur.Phys.J. **C18** (2001) 651.
- [6] M.M. Aggarwal et al., (WA93 Collaboration), Phys. Lett. **B404** (1997) 207.
- [7] H. Heiselberg, Phys. Rep. **351** (2001) 161.
- [8] M. Stephanov et al., Phys. Rev. Lett **81** (1998) 4816.
- [9] M.M. Aggarwal et al., (WA98 Collaboration), e-print: nucl-ex/0108029, Submitted to Phys. Rev. C.
- [10] K. Rajagopal and F. Wilczek Nucl. Phys. **B399** (1993) 395.
- [11] M.M. Aggarwal et al., (WA98 Collaboration), Phys. Rev. **C64** (2001) 011901(R).
- [12] D.P. Mahapatra, B. Mohanty and S.C. Phatak, Int. J. Mod. Phys.A in press, e-print: nucl-ex/0108011.
- [13] M.M. Aggarwal et al., To be published in Nucl. Instr. and Methods in Phys. Res. A, e-print: nucl-ex/0112016.